Proceedings of the 10^{th} Brazilian Congress of Thermal Sciences and Engineering – ENCIT 2004
Braz. Soc. of Mechanical Sciences and Engineering – ABCM, Rio de Janeiro, Brazil, Nov. 29 – Dec. 03, 2004

Paper CIT04-0417

A Study of the NSC2KE Finite Volume Method for Computing the Transonic Flow over a NACA 0012 Airfoil Inside a Wind Tunnel

Breno Moura Castro
Instituto de Aeronáutica e Espaço - IAE
Praça Mal. Eduardo Gomes, 50 - Jd. das Acácias
CEP: 12228-901 São José dos Campos - SP - Brazil
bmcastro@directnet.com.br

Abstract. *A numerical investigation of the transonic two-dimensional inviscid flow around a NACA 0012 profile inside a wind tunnel with height-to-airfoil chord of five is carried out using the NSC2KE finite-volume method. The upper-surface lift coefficients for zero incidence angle of attack and several transonic Mach numbers are compared with the results of Khalid and Mokry (1996). They solved the Euler equations for the same configuration using a finite-difference method and a structured grid. In the present investigation, two different unstructured meshes were used to assess grid sensitivity. The good agreement of the two methods shows that NSC2KE can yield reliable results for transonic wall interference problems.*

keywords: *Euler simulation, wind tunnel, interference, NSC2KE, NACA 0012.*

1. Introduction

Wall interference correction methods for transonic flows inside wind tunnels are still a challenge for researchers and scientists. Currently, the estimation of the effects of the tunnel walls on the flow around a model relies only on numerical methods.

It has been shown (Castro, 2001) that the interference of tunnel walls on unsteady flows in the transonic regime is quite substantial. Therefore, reliable tools for the transonic wall interference estimation are imperative. Computational Fluid Dynamics (CFD) reached a maturity level such that this method can provide the necessary reliability.

The use of structured grids for the discretization of the domain is more frequent than the use of unstructured ones. However, from the standpoint of allowing an easier discretization of complex geometries, the use of unstructured grids is preferable. Nonetheless, it appears that most of recent research on wind tunnel wall interference has been conducted with the aid of structured meshes. An example is the investigation performed by Khalid and Mokry (Khalid and Mokry, 1996).

The interference of tunnel walls in the subsonic regime has been extensively studied by many researchers. A classical work in this subject is Pope (Rae Jr. and Pope, 1984). Also important is the compilation made by Mokry (Mokry et al., 1980). A numerical approach for evaluating subsonic blockage corrections was developed by Castro (Castro, 1997), based on the panel technique.

This work is conducted using a Finite Element Method called NSC2KE (Mohammadi, 1994) for modeling the flow around a NACA 0012 airfoil inside a two-dimensional wind tunnel. The height of the tunnel is five times the chord of the airfoil which is in the center of the tunnel and parallel to the walls.

The Mach number of free-stream flow varies from 0.4 up to 1.4. The suction force coefficient on the upper part of the airfoil is compared with the results obtained by Khalid and Mokry (Khalid and Mokry, 1996). The good agreement between the two sets of data indicates that the NSC2KE yields reliable results for Euler computations. A grid sensitivity analysis was also carried out in the present work.

Khalid and Mokry also pointed out that their approach encountered no difficulties to compute lifting airfoil flows inside choked wind tunnels. Because the computation of such problems for viscous flows is a natural extension of the present investigation, a previous transonic inviscid flow around a lifting NACA 0012 profile inside a two-dimensional wind tunnel with height-to-airfoil chord of 5 was also computed.

The results achieved in the present work suggest that NSC2KE could be used for transonic wall interference evaluation. Further investigation should be carried out for viscous computations.

2. Theoretical Background

The code NSC2KE (Mohammadi, 1994) is an unstructured finite volume Galerkin method (Kwon and Bang, 2000). It is capable of simulating a wide range of flow speeds, from the subsonic to the hypersonic regimes, for two-dimensional and axi-symmetric configurations.

2.1. Governing equations

NSC2KE is based on the Reynolds-Averaged Navier-Stokes Equations in non-dimensional form:

$$\frac{\partial \rho}{\partial t} + \nabla.(\rho u) = 0 \tag{1}$$

$$\frac{\partial \rho u}{\partial t} + \nabla.(\rho u \times u) + \nabla p = \nabla.[(\mu + \mu_t)S] \tag{2}$$

$$\frac{\partial \rho E}{\partial t} + \nabla.[(\rho E + p)u] = \nabla.[(\mu + \mu_t)Su] + \nabla[(\kappa + \kappa_t)\nabla T] \tag{3}$$

with

$$\kappa = \frac{\gamma \mu}{Pr}, \qquad \kappa_t = \frac{\gamma \mu_t}{Pr_t}, \tag{4}$$

$$\gamma = 1.4, \qquad Pr = 0.72, \qquad Pr_t = 0.9. \tag{5}$$

where $\mu = 1/Re_{lam}$ corresponds to the inverse of laminar Reynolds number and is given by the Sutherland law:

$$\mu = \mu_\infty \left(\frac{T}{T_\infty}\right)^{1.5} \left(\frac{T_\infty + 110}{T + 110}\right) \tag{6}$$

and ∞ denotes reference (free-stream) quantities.

This study was carried out only for Euler computations. Therefore, viscous terms should vanish in Eqs. (2) and (3).

2.2. Boundary conditions

The NSC2KE code has four different types of boundary conditions: solid bodies, inflow and outflow weak boundaries, inlet profiles, and symmetry or slip boundaries.

2.2.1. Solid bodies

The solid body boundary condition enforces the flow tangency condition, $\vec{V}.\hat{n} = 0$, for inviscid cases and the no-slip condition, $\vec{V} = 0$, for viscous calculations. $\vec{V}$ is the velocity vector and $\hat{n}$ is the unit normal at the wall.

2.2.2. Inflow and outflow weak boundaries

The implementation of these boundary conditions use flux splitting in positive and negative parts, following the sign of the eigenvalues of the Jacobian matrix $A = \partial F/\partial W$. The term $W = (\rho, \rho u, \rho v, \rho E)^T$ is the usual vector of the conserved variables and F is the advective operator.

$$\int_{\Gamma_\infty} F.\hat{n}\, d\sigma = \int_{\Gamma_\infty} (A^+ W_{in} + A^- W_\infty).\hat{n}\, d\sigma, \tag{7}$$

where W_{in} is the computed (internal) value of the previous iteration and W_∞ the external value.

2.2.3. Inlet profiles

The inlet profile can be given as an input for internal flow computations. These data may be obtained either from experiments or another numerical simulation.

2.2.4. Symmetry or slip boundaries

The symmetry boundary condition is implemented in the same manner as the flow tangency condition, that is, $\vec{V}.\hat{n} = 0$. This condition may be applied for both inviscid and viscous computations.

2.3. Numerical Scheme

NSC2KE is a finite-volume, Galerkin, explicit algorithm. An upwind Osher (Osher and Chakravarthy, 1982), Roe (Roe, 1981), or Kinetic (Perthame, 1990) Riemann solver can be used for the convective part of the Reynolds-Averaged Navier-Stokes equations.

The scheme is second order accurate in space by means of a MUSCL like extension involving upwind and centered gradients. The numerical instabilities generated at regions with large gradients are treated with a Van Albada (Van Albada and Van Leer, 1984) type limiter. A four-stage Runge-Kutta scheme is used for the time integration.

2.4. Computational grids

The discretization of the domain is represented by a computational grid. The grid cells are generated by a code called EMC2 (Saltel and Hecht, 1995). This program generates triangles around the body and set up the grid file to be used with the code NSC2KE. The file contains the coordinates of the vertices of the triangles and also the connectivity of these vertices or nodes.

3. Results and Discussion

The code NSC2KE was applied to simulate a NACA 0012 airfoil inside a wind tunnel. This problem was first studied by Khalid and Mokry (Khalid and Mokry, 1996). Their approach to simulate the two-dimensional transonic flow over the airfoil inside the tunnel was based on a finite-difference method using Euler equations. The height of the tunnel corresponded to five times the chord of the airfoil.

Views of the computational grids used in the present work, in the vicinity of the airfoil, are presented in Figs. 1 and 2. Note that only the upper side of the geometry was modeled, taking advantage of the symmetry of the problem.

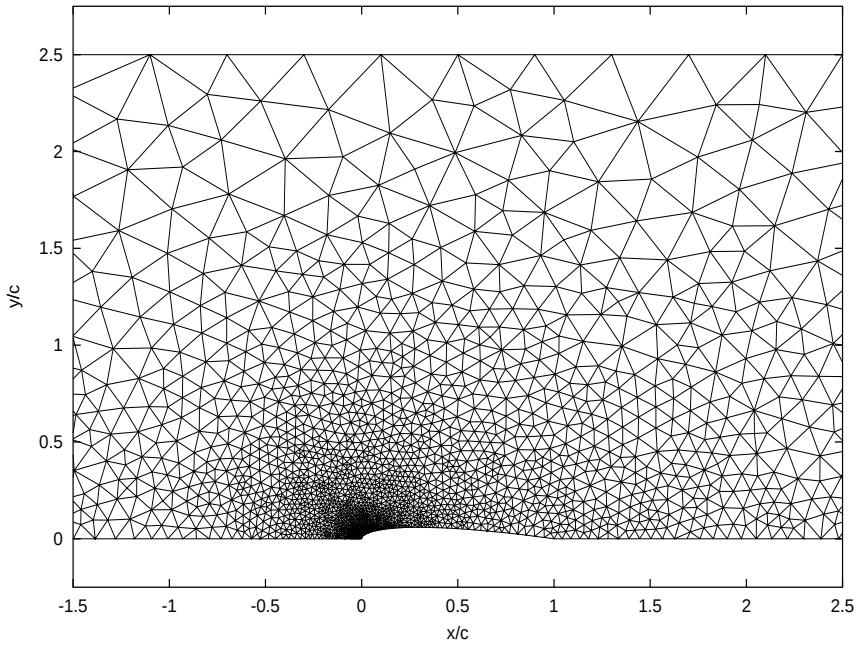

Figure 1: View of grid 1 in the vicinity of the airfoil

Grid 1 has 3,961 nodes and 7,598 triangles while grid 2 consists of 5,327 vertices and 10,300 cells. The flow tangency boundary condition is enforced on the surface of the airfoil and for the vertices on the tunnel wall, which corresponds to the line $y/c = 2.5$. The symmetry condition is applied for the nodes on the $y/c = 0$ line. For the nodes located at the inflow and outflow sections, the corresponding inflow and outflow weak boundary conditions are applied. Pressure was set to p_∞ for both inflow and outflow sections, meaning that there is no back pressure to drive the flow, in accordance with the simulations of Khalid and Mokry. The inflow section of the computational mesh was set to $x/c = -16$ and the outflow one to $x/c = 17$.

Computations were run for free-stream Mach numbers ranging from 0.5 to 1.35. All simulations were carried out on a Linux PC with a MMX 166 MHz Intel Pentium processor.

In order to compare results with Khalid and Mokry (Khalid and Mokry, 1996), the original NSC2KE source code was modified to compute and print the values of the aerodynamic coefficients c_D, c_L, and c_m. Khalid and Mokry calculated the suction force coefficient on the upper surface of the NACA 0012 airfoil, which they called c_L^u. As far as the domain used in this study corresponds to the upper side of the configuration only, the value of the c_L obtained here is equivalent to the value of upper-surface coefficient, c_L^u. Equation (8) translates the meaning of this coefficient.

$$c_L^u = -\frac{1}{c}\int_0^c c_p \, dx \tag{8}$$

Computed values of c_L^u are presented in Fig. 3 and Tab. (1). All computations were run until convergence was reached and all initial numerical disturbances were washed out from the domain.

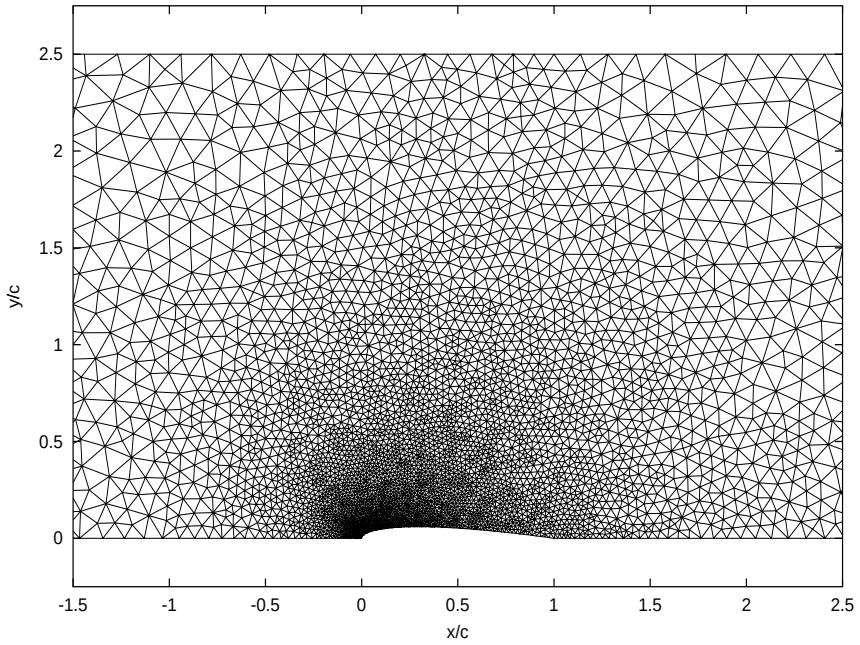

Figure 2: View of grid 2 in the vicinity of the airfoil

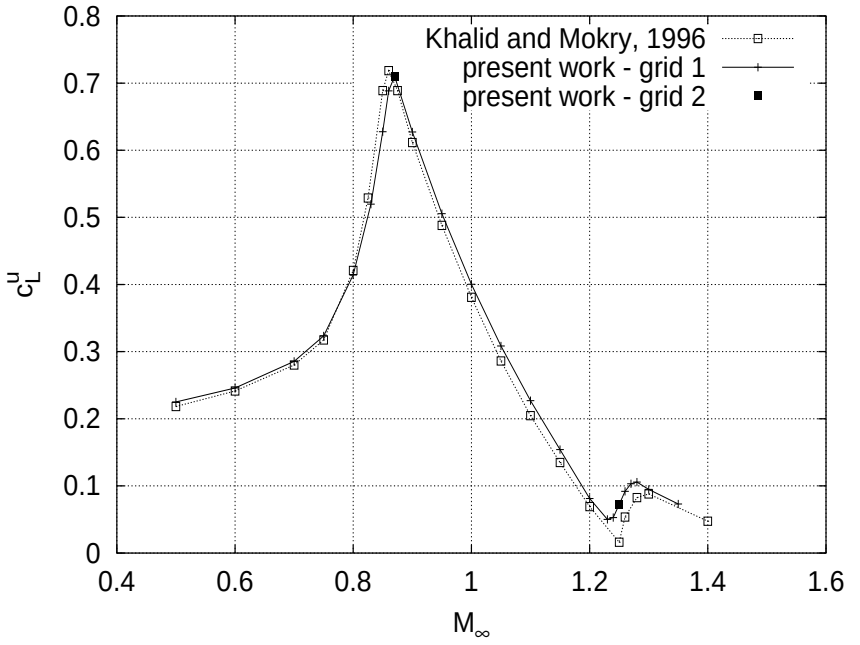

Figure 3: Upper lift coefficient comparison

Table 1: Computed values of c_L^u

M_∞	Grid 1	Grid 2
0.5	0.2250	
0.6	0.2459	
0.7	0.2855	
0.75	0.3234	
0.8	0.4142	
0.83	0.5198	
0.85	0.6277	
0.86	0.6884	
0.87	0.7101	0.7105
0.9	0.6271	
0.95	0.5055	
1.0	0.4003	
1.05	0.3085	
1.1	0.2270	
1.15	0.1541	
1.2	0.0813	
1.23	0.0501	
1.24	0.0528	
1.25	0.0723	0.0717
1.26	0.0919	
1.27	0.1031	
1.28	0.1057	
1.3	0.0949	
1.35	0.0731	

Simulations were run for grid 1 initially. The free-stream Mach number was varied from 0.5 to 1.35 in order to compare with the results of Khalid and Mokry. In their work, the O-type grid used in the computations had 161x33 points. There were 161 grid points on the surface of the NACA 0012 airfoil. Therefore, the upper surface had 80 segments or 81 node points. In present investigation, grid 1 and grid 2 contain 81 and 91 nodes over the upper surface of the airfoil, respectively.

The contour lines for the Mach number distribution for a free-stream Mach number $M_\infty = 0.87$ is shown in Fig. 4. This free-stream condition corresponds to the largest value of c_L^u. It can be seen that there is no shock over the surface of the airfoil. The oblique shock is at the trailing edge.

The Mach number field is presented in Fig. 5 for $M_\infty = 1.25$. This is the condition corresponding to the lowest c_L^u in Fig. 3. One can notice the detached shock wave in front of the airfoil.

Two extra simulations were performed with grid 2. The purpose was to verify grid sensitivity on the numerical solution. The chosen free-stream Mach numbers were 0.87 and 1.25. This choice was due to the peak observed at $M_\infty = 0.87$ and the discrepancy observed in Fig. 3, between the present and the results of Khalid and Mokry, around $M_\infty = 1.25$.

Observing the values presented in Tab. (1), the largest variation is less than 1%. Therefore, it is clear that the values of c_L^u shown here are not grid sensitive.

The reason for the discrepancy around $M_\infty = 1.25$ is believed to be due to the resolution of grids 1 and 2 near the leading edge of the airfoil.

According to Khalid and Mokry, the choking Mach numbers for a NACA 0012 profile inside a wind tunnel of a height-to-airfoil chord ratio of 5 are $M_{ch}^{(1)} = 0.837$ and $M_{ch}^{(2)} = 1.179$. The present results show the same characteristics observed by Khalid and Mokry over the choking interval. Furthermore, the slope of the c_L^u-curve at $M_\infty = 1$ is given by:

$$\left(\frac{\partial c_L^u}{\partial M_\infty}\right)_{M_\infty=1} = -\frac{4}{\gamma+1}\left[1 + \frac{1}{2}(c_L^u)_{M_\infty=1}\right] \tag{9}$$

Equation (9) was derived based on the sonic-freeze assumption. The $c_L^u = 0.4003$ for $M_\infty = 1$ yields a value for Eq. 9 of -2.00 ($\gamma = 1.4$). A numerical value for the slope of the c_L^u-curve at $M_\infty = 1$ can be obtained from the data shown in Tab. (1) using the following expression:

$$\left(\frac{\partial c_L^u}{\partial M_\infty}\right)_{M_\infty=1} \approx \frac{(c_L^u)_{i+1} - (c_L^u)_{i-1}}{(M_\infty)_{i+1} - (M_\infty)_{i-1}} \tag{10}$$

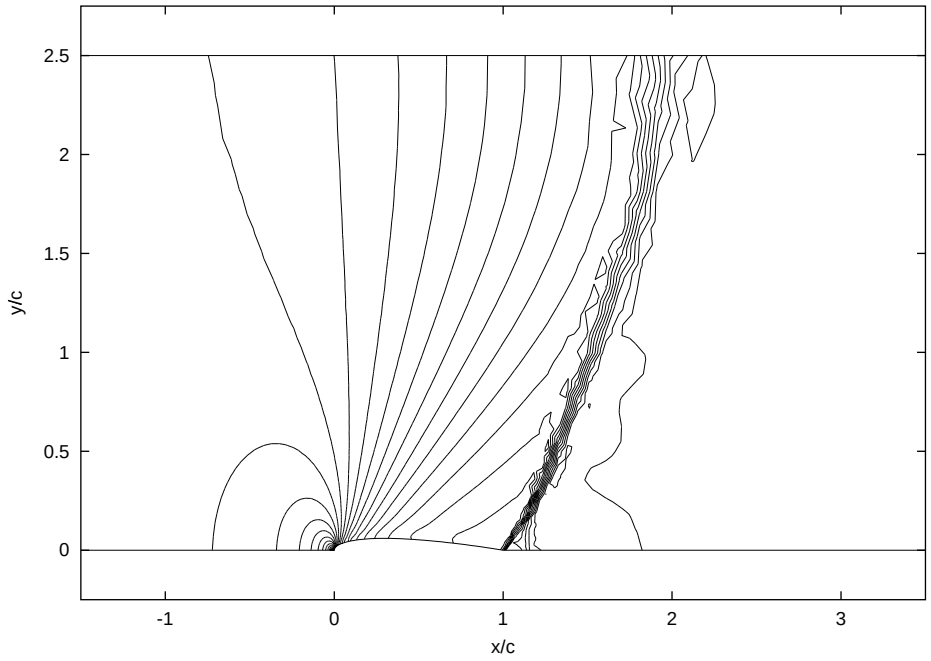

Figure 4: Mach number distribution for $M_\infty = 0.87$

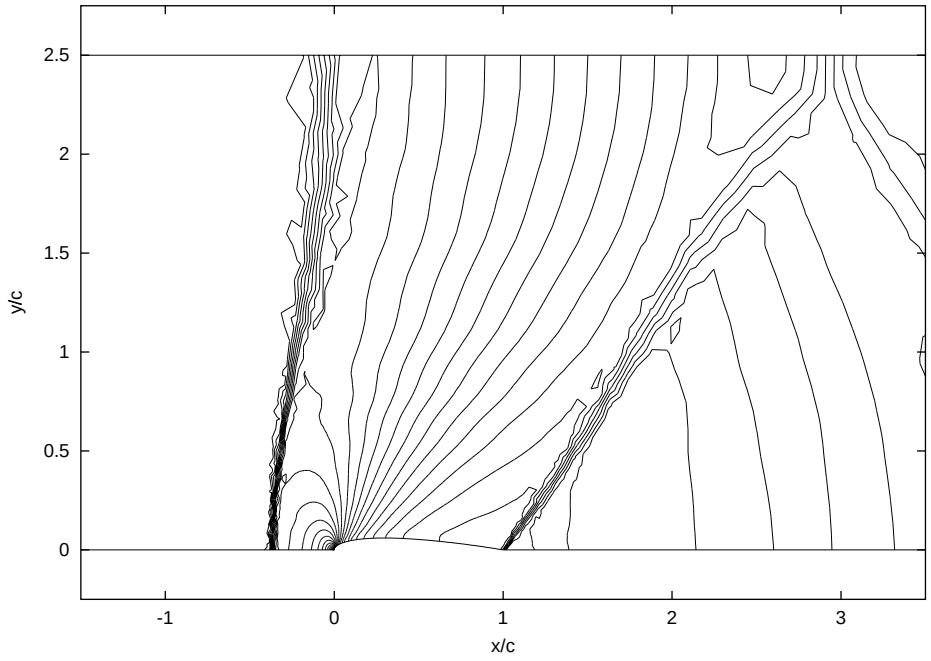

Figure 5: Mach number distribution for $M_\infty = 1.25$

where the indices $i+1$ and $i-1$ correspond to the points adjacent to $M_\infty = 1$.

Applying Eq. (10), the numerical value for the slope of the c_L^u-curve at $M_\infty = 1$ is -1.97. The values given by Eqs. (9) and (10) agree well in spite of the poor resolution of the c_L^u-curve around $M_\infty = 1$.

A lifting NACA 0012 airfoil inside a wind tunnel with the same height-to-airfoil ratio was also calculated for a free-stream Mach number of $M_\infty = 0.87$ and an angle of attack of $\alpha = 10^o$. The grid used for the Euler computation is presented in Fig. 6 and is formed by 12,672 nodes and 24,990 triangular cells.

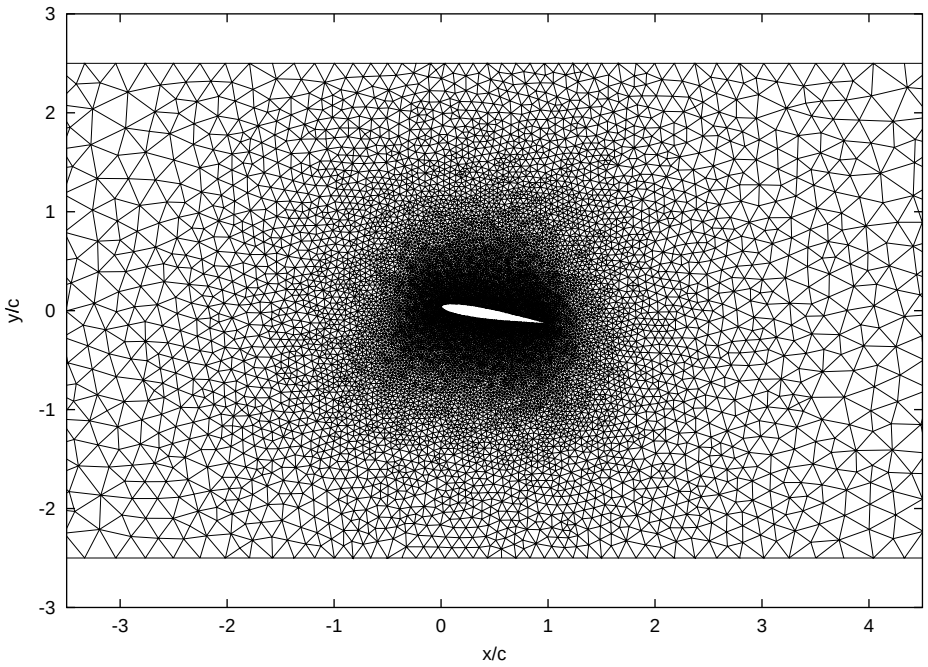

Figure 6: Grid in the vicinity of the NACA 0012 airfoil $\alpha = 10^o$

The Mach number distribution for the lifting profile simulation is shown in Fig. 7. The code was run up to a non-dimensional time of $t = 18.58$ in order to wash away all the initial numerical disturbances. This was sufficient to reduce the residual by more than three orders of magnitude. The time step was around $\Delta t = 0.00187$ and the CFL number was $CFL = 1$.

Consequently, it is observed that the NSC2KE finite volume method yields reliable results for Euler simulations of wind tunnel wall interference on transonic flows around a NACA 0012 airfoil at zero incidence. Additionally, the code was able to compute a confined transonic flow around a lifting profile.

Therefore, the investigation of viscous problems, using the NSC2KE code, is a natural continuation of the present work. Blockage effects over high incidence subsonic flows, supercritical airfoils inside slotted or perforated wind tunnels, and extreme ground effects are candidates for further studies.

4. Concluding Remarks

Several simulations were carried out for calculating inviscid transonic flows over a NACA 0012 profile inside a two-dimensional wind tunnel with solid walls. The height-to-airfoil chord ratio of the configuration was $h/c = 5.0$. The NSC2KE finite-volume method was used to perform the simulations.

Two computational meshes were used in order to evaluate grid sensitivity of the numerical solutions. Results for $M_\infty = 0.87$ and $M_\infty = 1.25$, near the limits of the choked flow range of the configuration, assure that the solutions were converged with respect to the spatial discretization.

Computations for free-stream Mach numbers ranging from $M_\infty = 0.5$ to $M_\infty = 1.35$ were compared with the results obtained by Khalid and Mokry (1996). The good agreement for the upper surface lift coefficient, c_L^u, indicates that NSC2KE yields reliable results for the estimation of transonic wall interference corrections.

Furthermore, the capability of NSC2KE to compute lifting airfoil simulations inside a choked wind tunnel was verified. This calculation was motivated by the intention to extend the present research to viscous problems.

Finally, the use of NSC2KE to estimate wind tunnel wall interference should be further investigated for viscous problems such as airfoils at high angles of attack and large blockage ratios, supercritical profiles inside perforated or slotted wind tunnels, and ground interference effects.

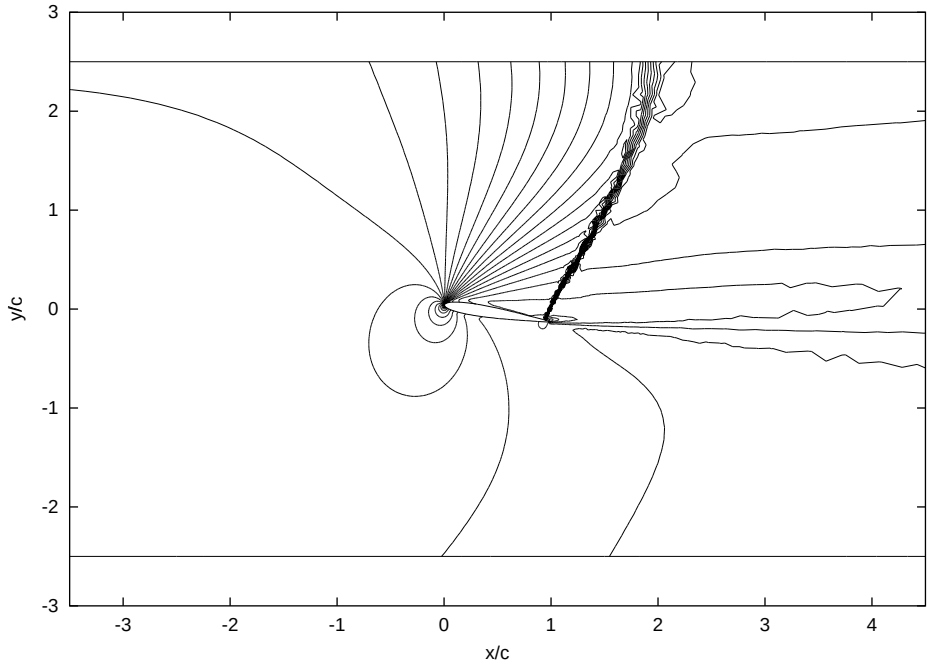

Figure 7: Mach number distribution for $M_\infty = 0.87$, $\alpha = 10^o$

5. References

Castro, B. M., 1997, Interferência das Paredes de um Túnel de Vento em Modelos Tridimensionais Complexos Utilizando o Método dos Painéis, Master's thesis, Instituto Tecnológico de Aeronáutica.

Castro, B. M., 2001, "Multi-Block Parallel Navier-Stokes Simulation of Unsteady Wind Tunnel and Ground Interference Effects", PhD thesis, Naval Postgraduate School, Monterey, CA.

Khalid, M. and Mokry, M., 1996, NPARC Study of a Two-Dimensional Transonic Wall Interference, "Journal of Aircraft", Vol. 33, No. 5, pp. 906–912.

Kwon, Y. W. and Bang, H., 2000, "The Finite Element Method Using MATLAB", CRC Press, 2 edition, ISBN 0849300967.

Mohammadi, B., 1994, Fluid Dynamics Computation with NSC2KE - An User Guide - Release 1.0, Technical Report RT-0164, INRIA.

Mokry, M., Chan, Y. Y., and Jones, D. J., 1980, Two-Dimensional Wind Tunnel Wall Interference, Technical Report 281, AGARDograph.

Osher, S. and Chakravarthy, S., 1982, Upwind Difference Schemes for the Hyperbolic Systems of Conservation Laws, "Mathematics of Computation", Vol. .

Perthame, B., 1990, Boltzmann Type Schemes for Gas Dynamics and Entropy Property, "SIAM Num. Anal.", Vol. 6, No. 27.

Rae Jr., W. H. and Pope, A., 1984, "Low-Speed Wind Tunnel Testing - 2nd Ed.", John Wiley & Sons, New York, ISBN 0-471-87402-7.

Roe, P. L., 1981, Approximate Riemann Solvers, Parameters, Vectors, and Difference Schemes, "Journal of Computational Physics", Vol. 43.

Saltel, E. and Hecht, F., 1995, EMC2 Wysiwyg 2D finite elements mesh generator, Technical Report 118, INRIA.

Van Albada, G. D. and Van Leer, B., 1984, Flux Vector Splitting and Runge-Kutta Methods for the Euler Equations, "ICASE 84-27".